Journal Name

ARTICLE

Electronic Supplementary Information (ESI)

Phenanthriplatin (IV) Conjugated Multifunctional Up-Converting Nanoparticles for Drug Delivery and Biomedical Imaging

Bo Teng,[a] Yanqiu Han,[b]* Xinyang Zhang,[c] Haihua Xiao,[d]* Chang Yu,[c] HeJie Li,[a] Ziyong Cheng,[c] Dayong Jin,[e] Ka-Leung Wong [f], Ping'an Ma,[a,c,]*and Jun Lin[c]

[a] Department of Otolaryngology Head and Neck Surgery, The Second Hospital, Jilin University, Changchun, 130041, China.

[b] Department of Neurology, The Second Hospital, Jilin University, Changchun, 130041, China. - Email: yanqiu9@hotmail.com

[c] State Key Laboratory of Rare Earth Resource Utilization, Changchun Institute of Applied Chemistry, Chinese Academy of Sciences, Changchun, 13002, P. R. China. E-mail: 就 jlin@ciac.ac.cn (Prof. Jun Lin) and mapa675@ciac.ac.cn (Dr. Ping'an Ma);

[d] Beijing National Laboratory for Molecular Sciences, State Key Laboratory of Polymer Physis and Chemistry, Institute of Chemistry, Chinese Academy of Sciences, Beijing 100190, P. R. China E-mail: hhxiao@iccas.ac.cn (Prof. Haihua Xiao)

[e] Institute for Biomedical Materials and Devices, Faculty of Science, University of Technology Sydney, NSW, 2007, Australia.

[f] Department of Chemistry, Hong Kong Baptist University, Kowloon Tong,Hong Kong

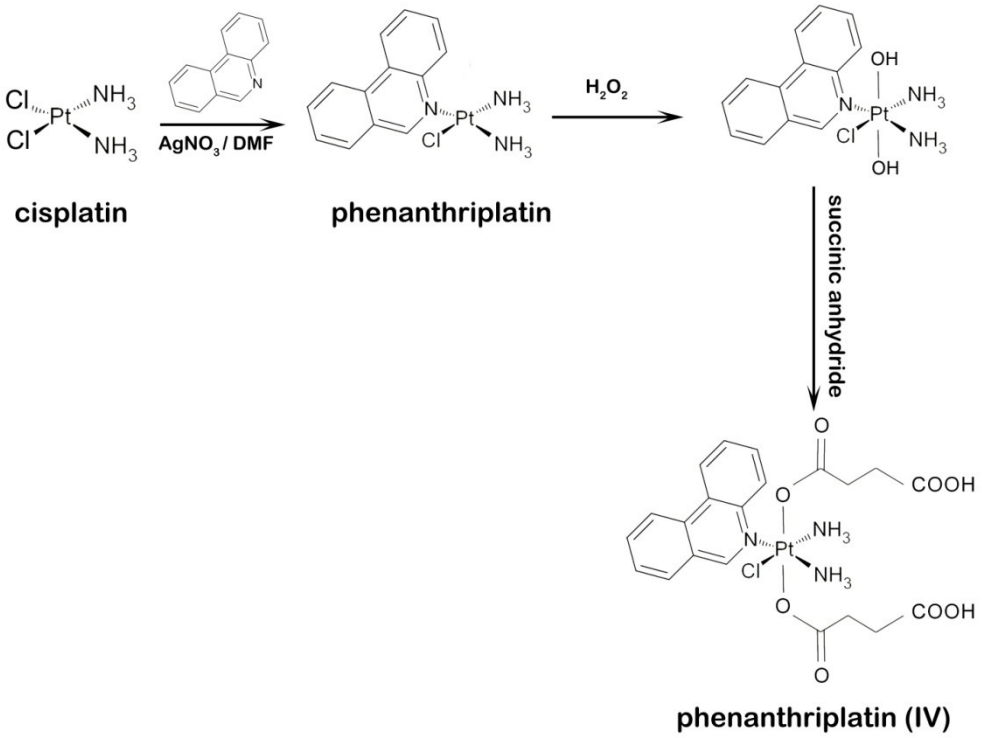

Figure S1. The detail synthesis process of phenanthriplatin (IV) [Phen-Pt (IV)].

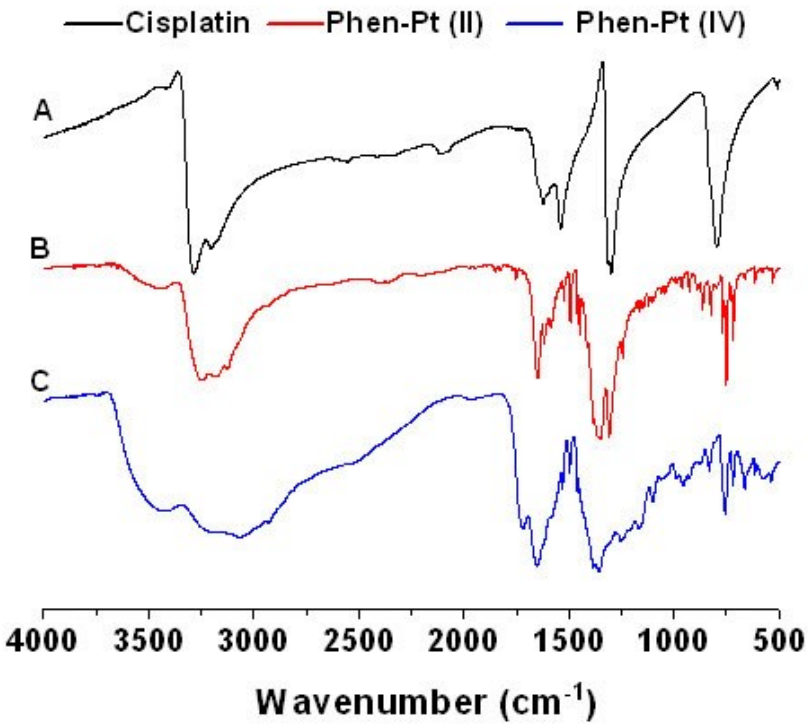

Figure S2. The FT-IR spectra of cisplatin (A), phenanthriplatin [Phen-Pt (II)] (B), phenanthriplatin (IV) [Phen-Pt (IV)](C).

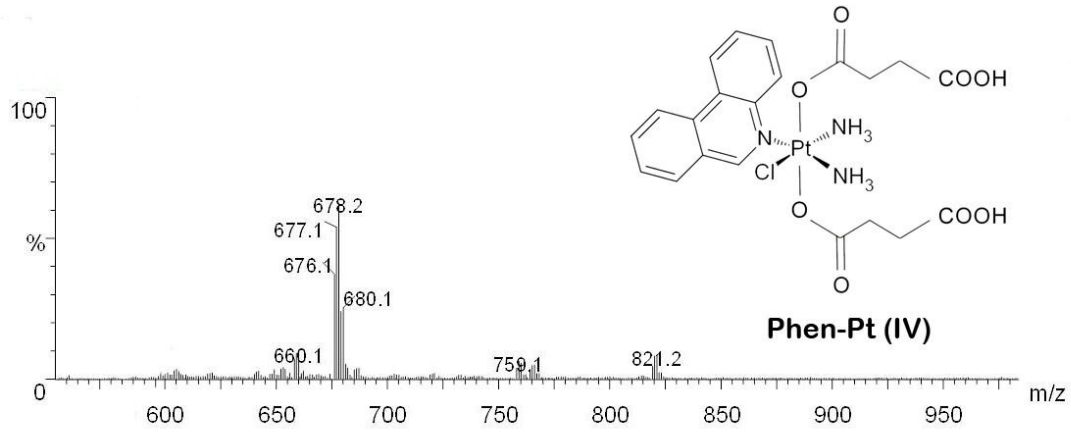

Figure S3. The mass spectra of Phen-Pt (IV).

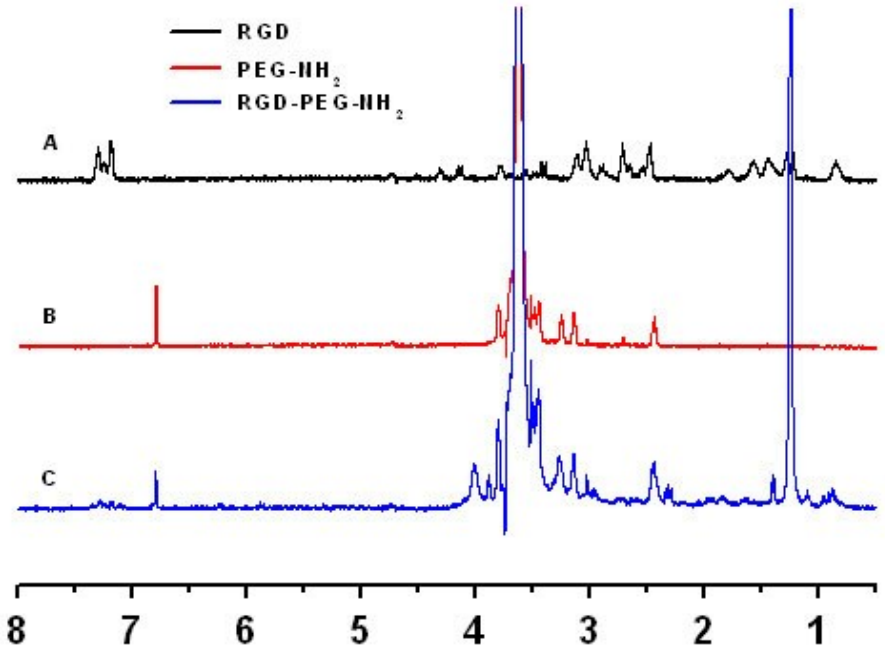

Figure S4. ^{1}H NMR spectrum of RGD (A), PEG-NH_2 (B), RGD-PEG-NH_2 (C).

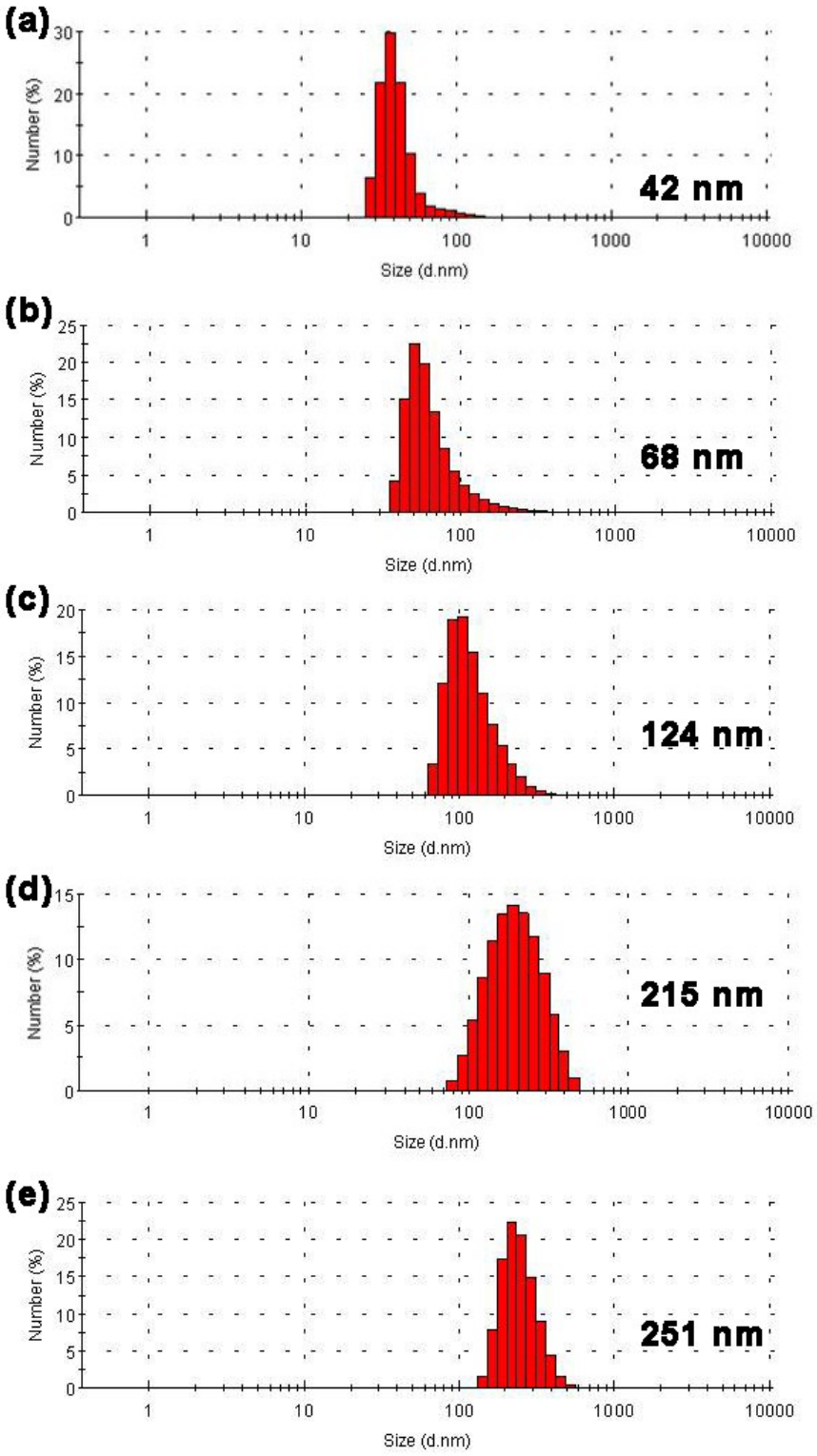

Figure S5. Particle size distribution of different nanoparticles in water. UCNPs(a), NP-1(b), NP-2(c), NP-3(d), and NP-4(e), determined by dynamic light scattering (DLS).

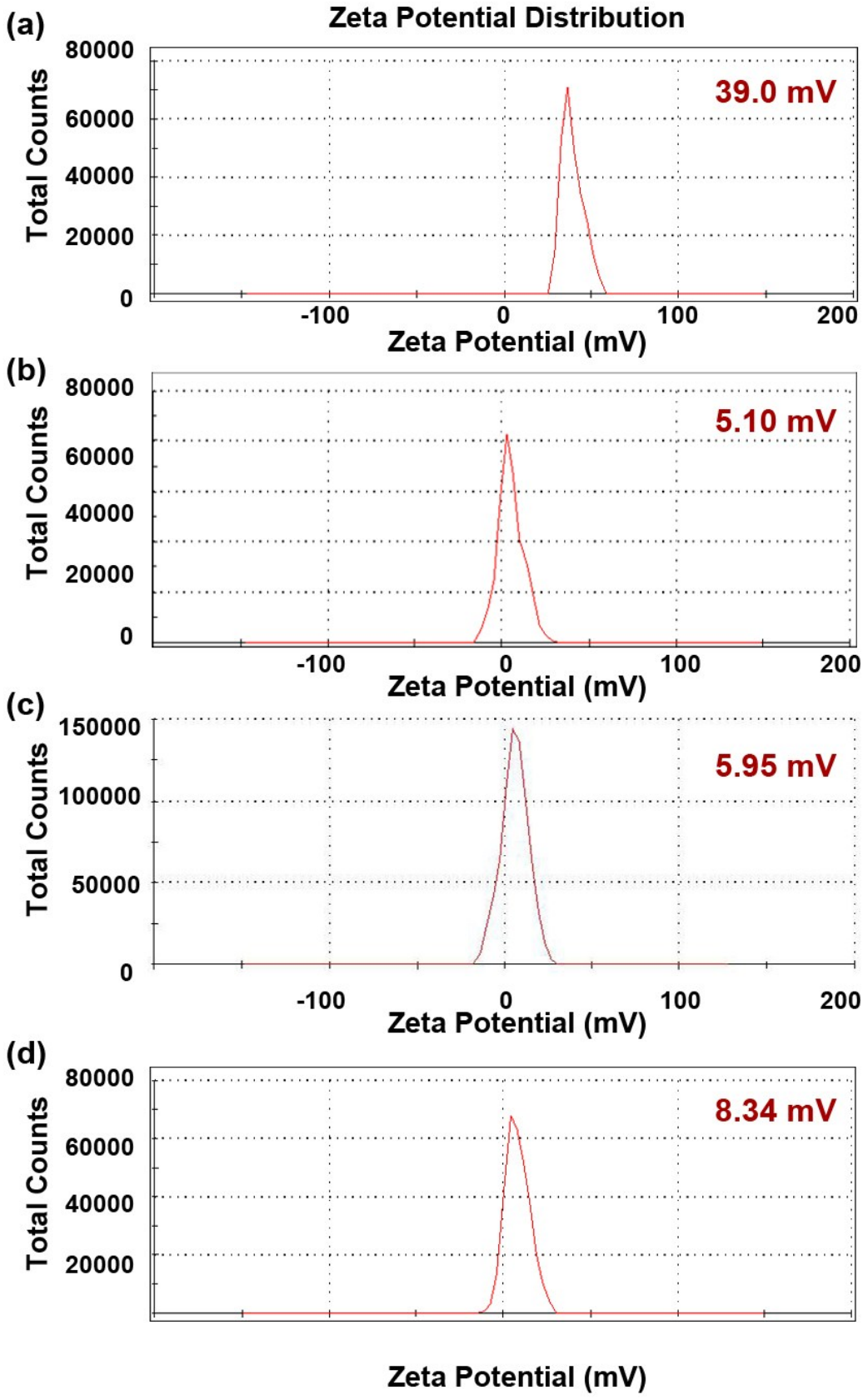

Figure S6. Zeta potential of different nanoparticles in water. UCNPs(a), NP-1(b), NP-2(c), NP-3(d), and NP-4(e), determined by dynamic light scattering (DLS).

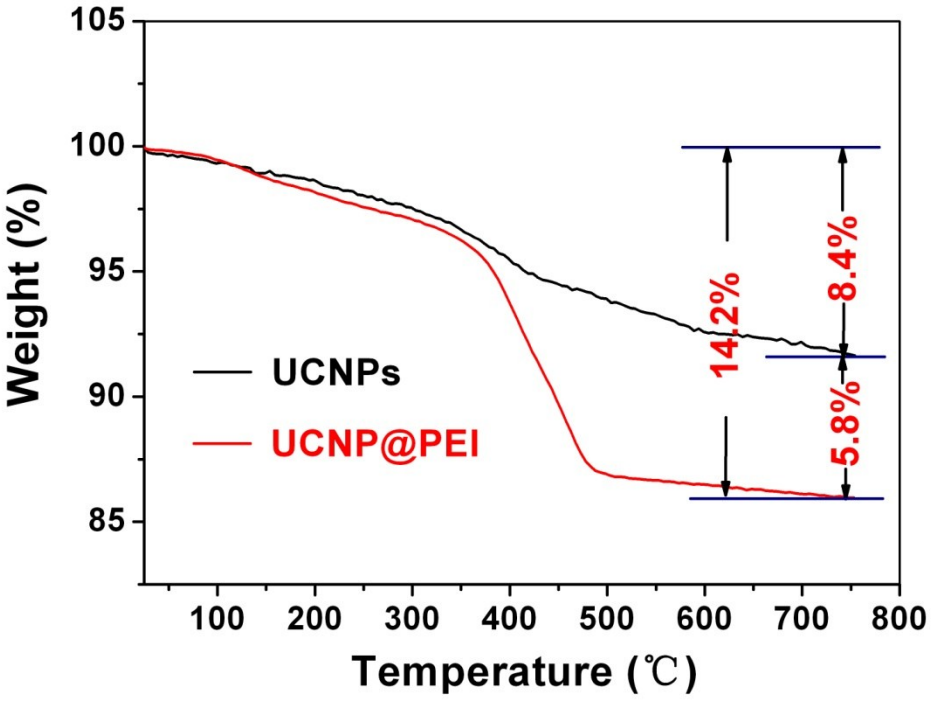

Figure S7. Thermogravimetric (TG) analysis of UCNPs and UCNP@PEI.

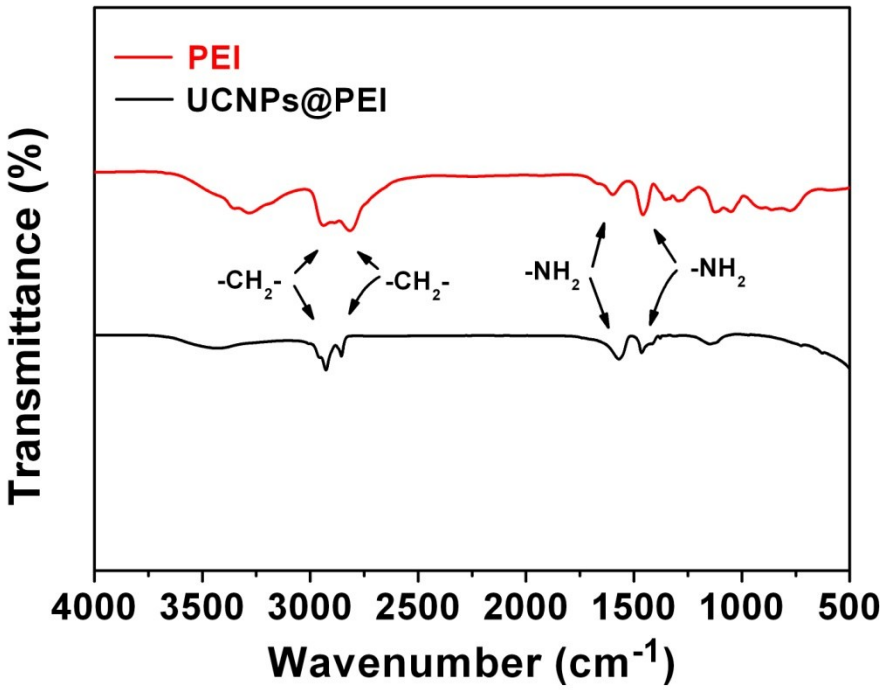

Figure S8. FT-IR spectra of PEI and UCNPs@PEI.

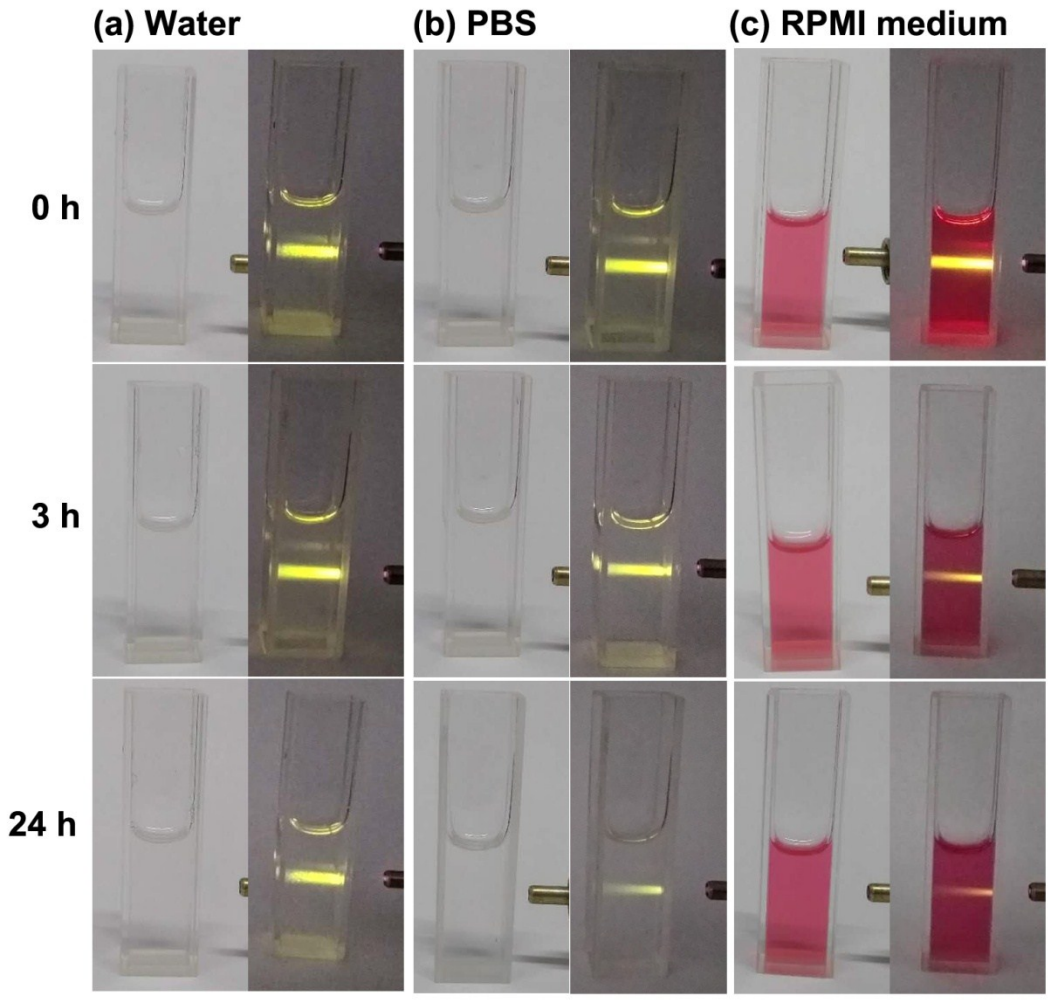

Figure S9. The colloidal stability and luminescence intensity of the NP-3 nanomaterials in different media at different times: (a) water; (b) PBS; (c) RPMI cell culture medium.

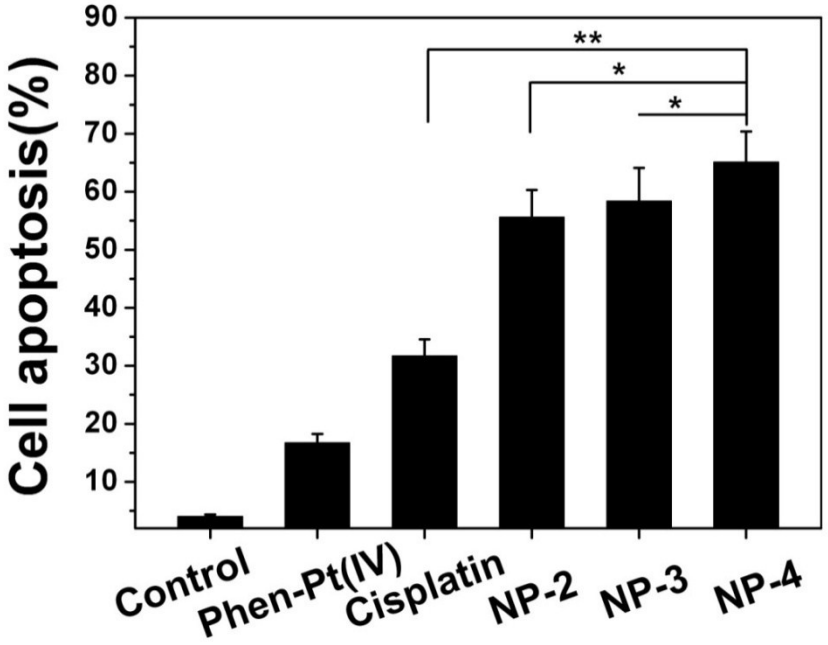

Figure S10. Flow cytometry apoptosis analysis of the Hep-2 cells incubated with control, Phen-Pt(IV), cisplatin, NP-2, NP-3, NP-4. The data are expressed as the mean ± standard deviation (n=3). Significance is indicated as *P<0.05 or **P<0.01

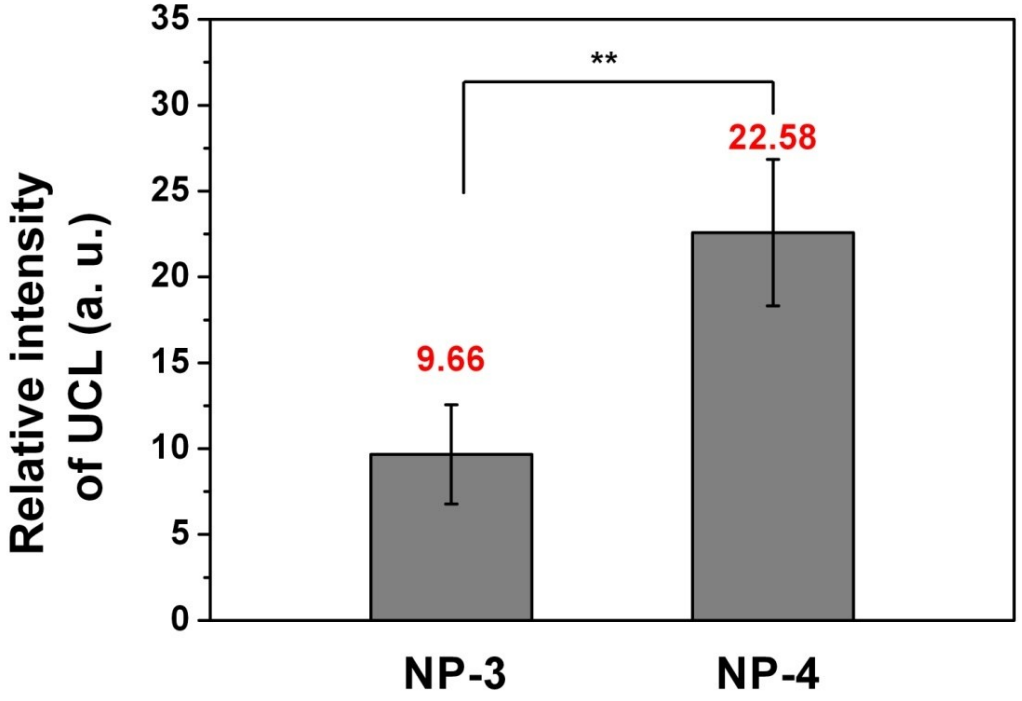

Figure S11. Relative intensity of tumour upconversion luminescent (UCL) imaging of NP-3 and NP-4. The data are expressed as the mean ± standard deviation (n=3). Significance is indicated as *P<0.05 or **P<0.01

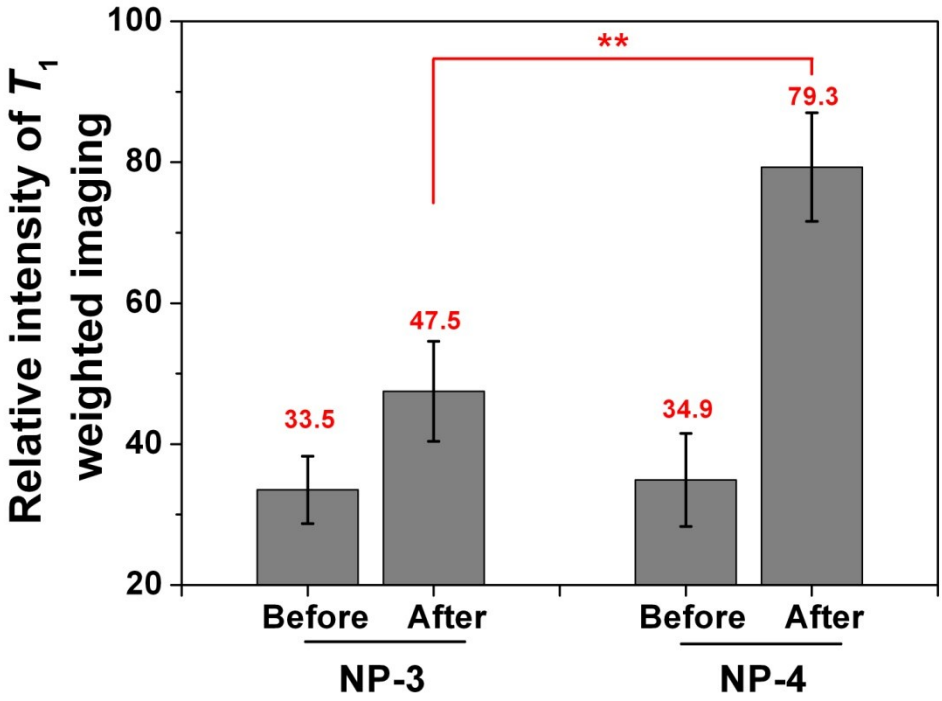

Figure S12. Relative intensity of T_1 weighted imaging of NP-3 and NP-4. The relative intensity was determined using densitometry scans to obtain quantitative data (Image J). The data are expressed as the mean ± standard deviation (n=3). Significance is indicated as *P<0.05 or **P<0.01

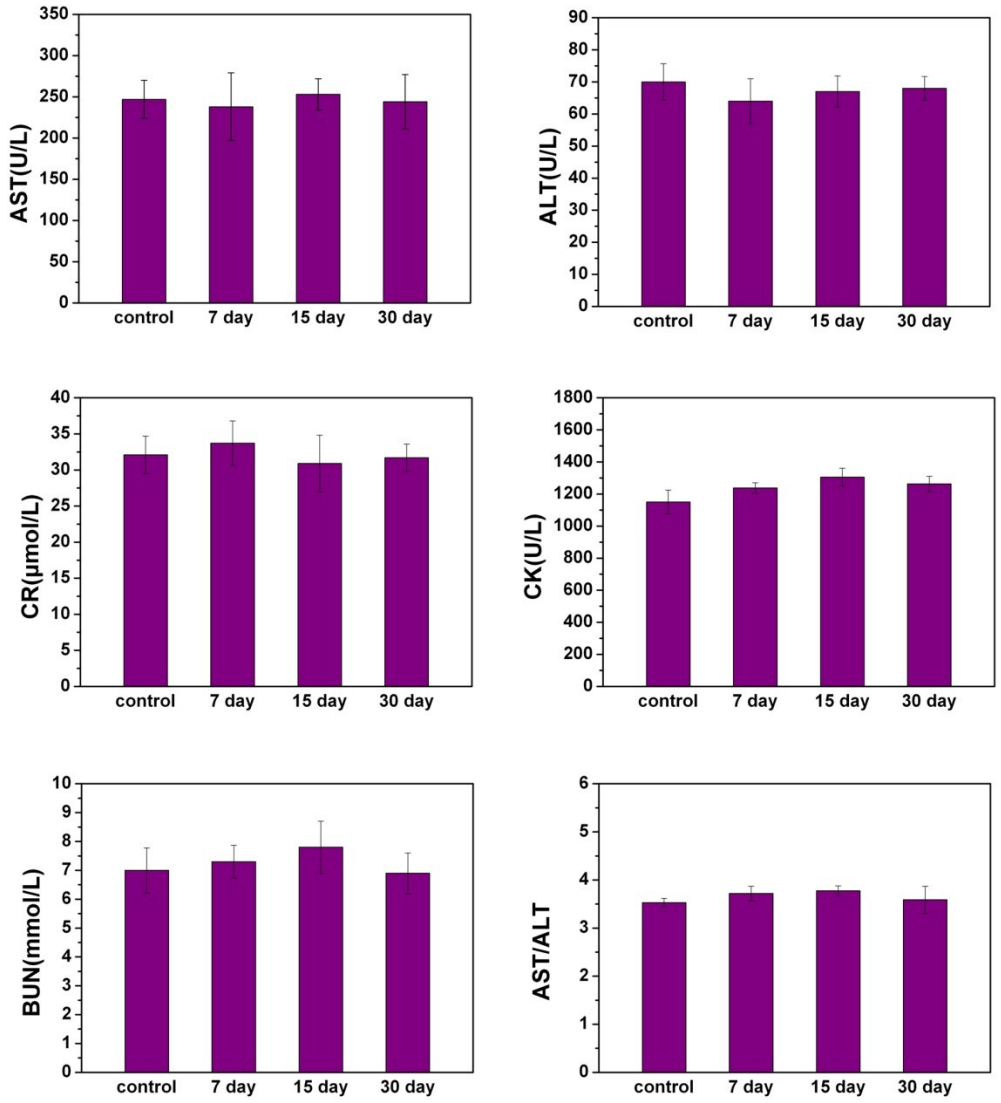

Figure S13. Blood analysis data of mice at 7 days, 15 days, and 30 days after NP3 treatment. All parameters of blood analysis including AST, ALT, AST/ALT, CR, CK and BUN fell well within the normal range. No significant difference in all blood test data. Error bars were based on three mice per group.